Biochimica et Biophysica Acta 1777 (2008) 1455–1462

Contents lists available at ScienceDirect

Biochimica et Biophysica Acta

journal homepage: www.elsevier.com/locate/bbabio

The *Toxoplasma gondii* type-II NADH dehydrogenase TgNDH2-I is inhibited by 1-hydroxy-2-alkyl-4(1H)quinolones

San San Lin [a], Stefan Kerscher [b], Ahmad Saleh [a], Ulrich Brandt [b], Uwe Groß [a], Wolfgang Bohne [a,*]

[a] *Institute of Medical Microbiology, University of Göttingen, Kreuzbergring 57, Göttingen D-37075, Germany*
[b] *Johann Wolfgang Goethe-Universität, Fachbereich Medizin, Zentrum der Biologischen Chemie, Molekulare Bioenergetik, Centre of Excellence Frankfurt "Macromolecular Complexes", Frankfurt am Main, Germany*

ARTICLE INFO

Article history:
Received 27 June 2008
Received in revised form 11 August 2008
Accepted 12 August 2008
Available online 22 August 2008

Keywords:
Alternative (type-II) NADH dehydrogenase (NDH2)
Toxoplasma gondii
Inhibition kinetics
Ping-pong mechanism
1-Hydroxy-2-alkyl-4(1)quinolone
HDQ

ABSTRACT

The apicomplexan parasite *Toxoplasma gondii* does not possess complex I of the mitochondrial respiratory chain, but has two genes encoding rotenone-insensitive, non-proton pumping type-II NADH dehydrogenases (NDH2s). The absence of such "alternative" NADH dehydrogenases in the human host defines these enzymes as potential drug targets. TgNDH2-I and TgNDH2-II are constitutively expressed in tachyzoites and bradyzoites and are localized to the mitochondrion as shown by epitope tagging. Functional expression of TgNDH2-I in the yeast *Yarrowia lipolytica* as an internal enzyme, with the active site facing the mitochondrial matrix, permitted growth in the presence of the complex I inhibitor DQA. Bisubstrate kinetics of TgNDH2-I measured within *Y. lipolytica* mitochondrial membrane preparations were in accordance with a ping-pong mechanism. Using inhibition kinetics we demonstrate here that 1-hydroxy-2-alkyl-4(1)quinolones with long alkyl chains of C_{12} (HDQ) and C_{14} are high affinity inhibitors for TgNDH2-I, while compounds with shorter side chains (C_5 and C_6) displayed significantly higher IC_{50} values. The efficiency of the various quinolone derivatives to inhibit TgNDH2-I enzyme activity mirrors their inhibitory potency *in vivo*, suggesting that a long acyl site chain is critical for the inhibitory potential of these compounds.

© 2008 Elsevier B.V. All rights reserved.

1. Introduction

NADH:ubiquinone oxidoreductases, also known as NADH dehydrogenases constitute one of the electron entry points into the respiratory chain, oxidizing NADH and generating ubiquinol. In eukaryotes, this class of enzymes is divided into two major subfamilies, which can be discriminated on the basis of cofactor content and sensitivity towards rotenone into type-I NADH dehydrogenases (complex I) and type-II NADH dehydrogenases (NDH2s) [1]. Proton-pumping complex I is a nearly ubiquitous enzyme that couples the rotenone-sensitive transfer of electrons from NADH to ubiquinone with the active transport of protons across the inner mitochondrial membrane [2]. Bacterial complex I typically consists of fourteen subunits that are homologous to the seven mitochondrially coded and the seven nuclear coded "central" subunits of the eukaryotic enzyme. Although eukaryotic complex I contains a variable number of so-called accessory subunits, with a total of 45 subunits and a molecular mass of roughly 1 MDa in mammals, the bioenergetic function and the overall structure are conserved [3,4].

In contrast to complex I, type-II NADH dehydrogenases are non-proton-pumping, rotenone-insensitive, single polypeptides. Their active site can face either to the cytosol (external enzymes), thereby oxidizing cytosolic NADH, or to the mitochondrial matrix (internal enzymes), thereby oxidizing mitochondrial NADH. Seven NDH2 isoforms are expressed in *Arabidopsis*, three of them are identified as internal enzymes, whereas the other four are external [5]. In *Saccharomyces cerevisiae* mitochondria lacking complex I, one internal and two external enzymes have been described [6].

Type-II NADH dehydrogenases have been described in plants, fungi, protozoa and bacteria [1,7], but appear to be absent in mammals, which qualifies them as attractive drug targets. The apicomplexan parasites *Plasmodium falciparum* and *Toxoplasma gondii*, which are the causative agents of malaria and toxoplasmosis respectively, both lack complex I. Instead, the genome of *P. falciparum* is predicted to encode a single NDH2 of unknown orientation, while the *T. gondii* genome encodes two NDH2 isoforms. Treatment of *P. falciparum* with micromolar concentrations of diphenylene iodonium chloride, a low affinity inhibitor of NDH2, resulted in an inhibition of PfNDH2 activity, in a collapse of the parasite's mitochondrial membrane potential and finally in parasite death [8].

Abbreviations: HFF, human foreskin fibroblasts; HDQ, 1-Hydroxy-2-Dodecyl-4(1H) Quinolone; HHQ, 1-Hydroxy-2-Hexyl-4(1H)Quinolone; HPQ, 1-Hydroxy-2-Pentyl-4 (1H)Quinolone; HTQ, 1-Hydroxy-2-Tetradecyl-4(1H)Quinolone

* Corresponding author. Tel.: +49 551 395869; fax: +49 551 395861.
E-mail address: wbohne@gwdg.de (W. Bohne).

0005-2728/$ – see front matter © 2008 Elsevier B.V. All rights reserved.
doi:10.1016/j.bbabio.2008.08.006

The quinolone-like compound 1-hydroxy-2-dodecyl-4(1)quinolone (HDQ) was described as the first high affinity inhibitor of type-II NADH dehydrogenases that inhibits NDH2 activity in mitochondrial membranes of the yeast *Yarrowia lipolytica* with an IC_{50} of 200 nM [9]. We have recently shown that HDQ is highly effective against *T. gondii* and inhibits parasite replication with an IC_{50} in the nanomolar range [10]. Moreover, a combined treatment of HDQ with the complex III inhibitor atovaquone resulted in synergism [10].

To further elucidate the suitability of type-II NADH dehydrogenases as drug targets it is crucial to obtain functional data from pathogen orthologs and to determine their interaction with putative inhibitors. We here report functional expression of TgNDH2-I in the yeast *Y. lipolytica*. This allowed us to study the kinetics of this enzyme and to demonstrate that 1-hydroxy-2-alkyl-4(1)quinolones with long alkyl side chains are high affinity inhibitors for TgNDH2-I.

2. Materials and methods

2.1. Genome data mining and sequence analyses

Preliminary genomic and/or cDNA sequence data were accessed via http://ToxoDB.org (version 3.0) [11] and/or http://tigr.org/tdb/t_gondii/. Genomic data were provided by the Institute for Genomic Research (NIH grant #AI05093), and by the Sanger Center (Wellcome Trust). EST sequences were generated by Washington University (NIH grant #1R01AI045806-01A1). Bioinformatics programs including MitoProt II 3.0 (http://ihg.gsf.de/ihg/mitoprot.html) and SignalIP 3.0 (http://ww.cgs.dtu.dk/services/SignalIP/) were used to predict subcellular location of *Tgndh-I* and *Tgndh2-II*.

2.2. Determination of the ATG initiation codons

An in-frame stop codon is present at 783 and 51 nt upstream of the presumed initiation ATG codons of *tgndh2-I* and *tgndh2-II* respectively. The deduced amino acid sequences coded by these regions have no other in-frame methionine residues and no similarity to NDHs nor to other proteins when blasted using NCBI BLAST. For *tgndh2-I* the next methionine residue is located 177 nt downstream of the first one. However, only the amino acid sequence deduced from the first ATG has characteristics of a mitochondrial targeting sequence. For *tgndh2-II*, a putative second start ATG is located 6 nt downstream of the first.

2.3. RNA extraction, RT-PCR and fusion-PCR

Total RNA was isolated using the GenElute Mammalian Total RNA Kit (Sigma) and treated with DNase I (Sigma). Reverse transcription (RT) was done on 5 μg of total RNA, Oligo(dT) primer (Sigma) and M-MLV reverse transcriptase (RNase H minus, Sigma) according to the manufacturer's instructions. For PCR amplification, the reaction mixture was cycled in a thermal cycler. Fusion-PCR amplification was firstly performed in a volume of 50 μl containing 50 ng of each purified DNA fragment (QIAquick PCR purification kit, Qiagen) with 5 cycles of PCR in the absence of primers. The PCR reaction was continued for another 7 cycles after adding the primer sets (BamHI-NUAM-Fusion+ with NDH2-I-FL− or NDH2-II-FL−).

2.4. Real-time PCR

Light cycler PCR (Roche) was performed to amplify cDNA of *tgndh2-I*, *tgndh2-II* and β-tubulin with the following primer sets RT-AND1/1+ and 2−, RT-AND2/1+ and 2−, and RT-Tub/3+ and 4−, as listed in Supplementary Table 1. A control sample without reverse transcriptase was incubated in parallel. The threshold crossing-point values of *tgndh2-I* and *tgndh2-II* were normalized to that of β-tubulin.

2.5. Immunofluorescence microscopy

Samples were fixed with 4% paraformaldehyde/PBS for 10 min and permeabilized with 0.25% Triton X-100/PBS for 15 min. After blocking for 1 h with 1% BSA/PBS, samples were incubated with a 1:250 dilution of anti-myc mAb 9E10 (Sigma) followed by incubation with a 1:500 dilution of Cy3-conjugated anti-mouse IgG (Dianova) in 1% BSA/PBS for 1 h each.

2.6. T. gondii strains, cultivation and in vitro stage conversion

Parasites were propagated in human foreskin fibroblasts (HFF) as previously described [12]. A clonal isolate of the RH strain was used for *in vitro* stage conversion and preparation of cDNA for real time RT-PCR analysis. Transactivator expressing *T. gondii* of strain RH TATi-1 [13] were kindly provided by Dr. D. Soldati and Dr. M. Meissner and used for transfection experiments. Bradyzoites obtained by *in vitro* stage conversion were prepared as follows. *T. gondii* infected HFFs were firstly cultivated in 1% FCS/DMEM for 3 h at 37 °C in a 5% CO_2 humidified atmosphere. The medium was subsequently replaced with pH-shift medium (pH 8.3) to induce bradyzoite differentiation [14] and the cultures were incubated at 37 °C without CO_2. The medium was changed daily with fresh pH-shift medium to remove the extracellular parasites and maintain a constant culture pH. After 4-day incubation, cells were detached and harvested for RNA isolation.

2.7. Generation of myc-tagged Tgndh2-I and Tgndh2-II for expression in parasites

The complete open reading frames (ORF) of *Tgndh2-I* and *Tgndh2-II* were amplified from cDNA of the RH strain using *Pfu* polymerase (Promega) with the primer sets AND1/ORF1+_AflII and AND1/ORF2−_AvrII, and AND2/ORF1+_NsiI and AND2/ORF2_AvrII, respectively. The PCR fragments were cloned into pCR4.0-TOPO (Invitrogen) and DNA sequenced. The AflII/AvrII and NsiI/AvrII fragments were finally subcloned into pTetO7Sag4-acyl carrier protein (ACP)-cmyc-DHFR vector (kindly provided by Dr. B. Striepen), thereby replacing the ACP ORF with the *Tgndh2-I* and *Tgndh2-II* ORFs. The final constructs pTetSag4-ndh2-I-cmyc-DHFR and pTet7Sag4-ndh2-II-cmyc-DHFR consisted of the anhydrotetracycline (Atc)-regulable TetO7Sag4 promoter element [15], which controls the expression of the complete *Tgndh2-I* and *Tgndh2-II* ORFs with a C-terminal myc-tag, and additionally includes a pyrimethamine resistance cassette for selection [16]. Parasites (2×10^7) were electroporated with 50 μg of NotI-linearized constructs as previously described [12]. Not I (25 U) was added to the cytomix before electroporation in order to increase the frequency of stable transfectants [17]. Stably transfected parasites were selected with 1 μM pyrimethamine.

2.8. Plasmid construction and Y. lipolytica transformation

The NUAM-*Tgndh2s* fusion constructs were generated as translational fusions comprising the *Y. lipolytica* mitochondrial targeting sequence of the complex I NUAM subunit [18] and the corresponding *Tgndh2-I* or *Tgndh2-II* mature peptides. The NUAM DNA fragments were amplified by PCR from plasmid pUB38 [19] using proof-reading Phusion DNA polymerase (Finnzymes' Phusion high-fidelity DNA polymerase, NEB) with sense primer BamHI-NUAM-Fusion+ and the corresponding antisense primers YL-NDH2-I-24−, YL-NDH2-I-51− and YL-NDH2-II-62− (Supplementary Table S1). For obtaining DNA fragments for the mature parts of the *Tgndh2-I*-(*AA24*), *Tgndh2-I*-(*AA51*) and *Tgndh2-II*-(*AA62*) constructs, cDNA isolated from the RH strain was used as a template for PCR amplification with the following primer sets: YL-NDH2-I-24+ and NDH2-I-FL−, YL-NDH2-I-51+ and NDH2-I-FL, and YL-NDH2-II-62+ and NDH2-II-FL−, respectively. The NUAM-*Tgndh2* fusions were achieved by fusion-PCR. To create the

*Tgndh2*s full-length constructs, primer sets NDH2-I-FL+ and NDH2-I-FL− for *Tgndh2-I*, and NDH2-II-FL+ and NDH2-II-FL− for *Tgndh2-II* were used as shown in Supplementary Table S1. All PCR fragments were cloned into pDrive vector (PCR cloning kit, Qiagen) according to the manufacture's protocol, and then subcloned into the BamHI and EcoRI sites of the *Y. lipolytica*/*E. coli* shuttle vector pUB30 [19], behind the pPOX2 promoter. All clones were sequenced and confirmed with correct orientation. *Y. lipolytica* haploid *NDH2* deletion strain GB5.2 [20] was used for transformation with pUB30 constructs encoding TgNDH2-I and TgNDH2-II full-length, or NUAM-TgNDH2-I and NUAM-TgNDH2-II fusion constructs. Transformants were grown in rich glucose medium in the presence of 100 μg/ml Hygromycin B.

2.9. Preparation of mitochondrial membranes

Mitochondrial membranes were isolated as previously described [9]. In brief, cells were harvested and resuspended in ice-cold buffer containing 600 mM sucrose, 20 mM Na^+/Mops, pH 7.4, 1 mM EDTA, and 2 mM phenyl-methylsulfonyl fluoride, and disrupted by glass beads. Mitochondrial membranes were collected from the supernatant and further homogenized, shock-frozen and stored at −80 °C. Samples were aliquoted for kinetic measurements and protein determination.

2.10. Kinetic measurements

NADH:DBQ oxidoreductase activity of mitochondrial membranes from *Y. lipolytica* expressing *Tgndh2-I* and *Tgndh2-II* was measured at 30 °C in a reaction mixture containing 20 mM Na^+/Mops (pH 7.4), 50 mM NaCl, 2 mM KCN, 0.1 μM NADH, 60 μM DBQ, and 100 μg/ml mitochondrial membranes in the presence of 27 μM complex I inhibitor DQA. The reaction was initiated by adding DBQ and monitored using a plate reader spectrophotometer (SPECTRAmax PLUS 384, Molecular Devices). Enzyme activities were recorded in terms of velocity (v, unit: $\mu M \cdot min^{-1} \cdot mg^{-1}$). The applied DBQ concentrations were in the range from 2.5–100 μM (at 100 μM NADH) and the NADH concentrations were in the range from 10–100 μM (at 60 μM DBQ). Data were analysed according to the equations detailed in [9]. Determination of Michaelis–Menten parameters was by direct fit using the ENZFITTER software package (Biosoft, Cambridge). HDQ and HDQ analogues were kindly provided by Dr. W. Oettmeier and were dissolved in tissue culture grade DMSO (Sigma).

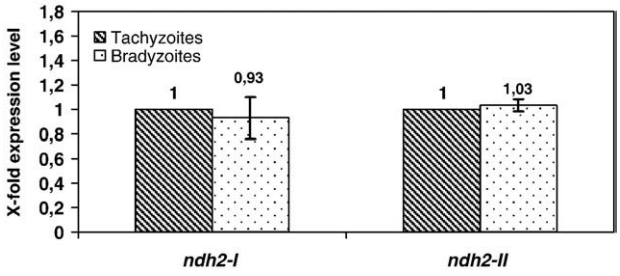

Fig. 2. Real-time PCR analysis for TgNDH2-I and TgNDH2-II mRNA transcripts. HFFs were infected with RH strain tachyzoites in alkaline medium of pH 8.3 to induce bradyzoite differentiation. Total RNA was isolated from tachyzoites at 24 h post-infection and from bradyzoites at 4 days post-infection. Light cycler PCR was performed to amplify cDNAs of TgNDH2-I and TgNDH2-II. β-tubulin was used as an internal control. Values are represented in terms of x-fold increase in the mRNA transcripts of TgNDH2-I and TgNDH2-II in tachyzoites compared to that in bradyzoites after normalization to β-tubulin mRNA transcripts. Results are expressed as mean ± S.D. of the duplicate wells of two independent experiments.

2.11. Nucleotide sequence accession numbers of Tgndh2-I and Tgndh2-II genes

Sequence data of *Tgndh2-I* and *Tgndh2-II* were submitted to GenBank with accession numbers DQ211932 and DQ228957, respectively.

3. Results

3.1. T. gondii expresses two mitochondrial NDH2 isoforms but no complex I

Based on BLAST homology searches, the genome of *T. gondii* is predicted to encode conventional respiratory chain components, with the exception of the multi-subunit, proton-translocating NADH

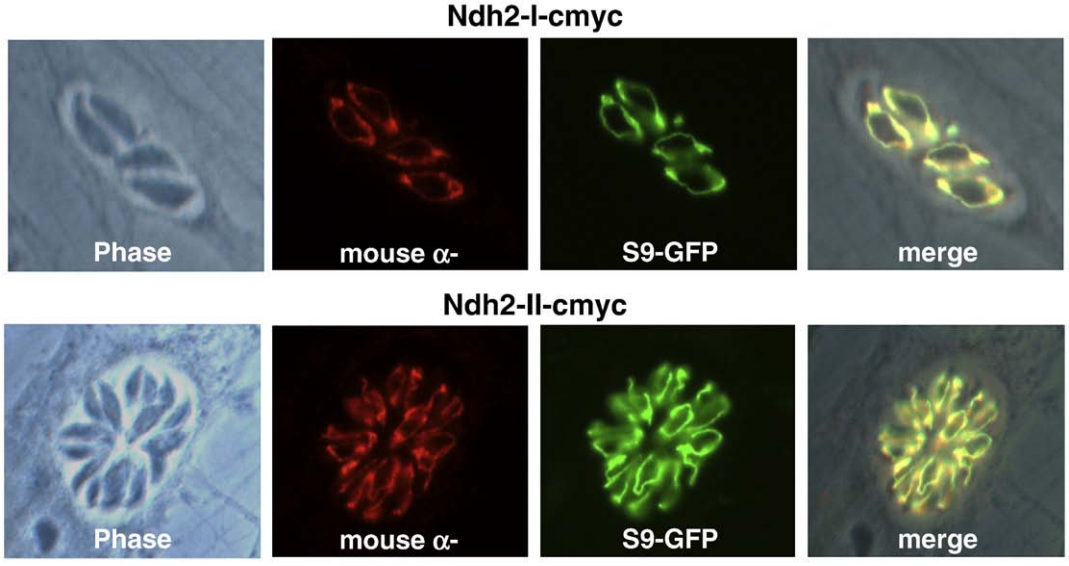

Fig. 1. Mitochondrial localization of myc-tagged TgNDH2-I and TgNDH2-II in parasites. RH strain tachyzoites were transfected with expression plasmids (pTetO7Sag4-NDH2-I/II-cmyc-DHFR), harboring the complete ORFs of TgNDH2-I and TgNDH2-II. The myc-tagged fusion proteins were detected by immunofluorescence staining using anti-myc mAB 9E10. For co-localization experiments, stably transfected parasites expressing the ectopic TgNDH2-I and TgNDH2-II genes were co-transfected with pCAT S9-GFP, which encodes a mitochondrially targeted GFP fusion.

dehydrogenase known as complex I. Instead, two contigs (TGG_994254 and TGG_994290) with high similarities to type-II NADH dehydrogenases were identified in the ToxoDB. The complete open reading frames of both genes were amplified, subcloned and sequenced from *T. gondii* RH strain cDNA. The two genes encoding the type-II NADH dehydrogenases were designated as *tgndh2-I* (accession#: DQ211932) and *tgndh2-II* (accession#: DQ228957). They encode precursor polypeptides of 619 and 657 amino acids with predicted masses of 67.1 and 72.1 kDa, respectively. Information on gene structures is given in Supplementary Fig. S1. The deduced primary structure of both proteins includes N-terminal mitochondrial targeting sequences as predicted by MitoProt II and SignalP 3.0. To verify the mitochondrial localization of *Tg*NDH2-I and *Tg*NDH2-II, we performed epitope tagging experiments. The complete open reading frames (ORF) of both genes were fused to a C-terminally located c-myc epitope and the resulting expression plasmids (pTetO7Sag4-NDH2-I/II-cmyc-DHFR) were introduced into RH strain parasites of the TATi-1 line by electroporation. Immunofluorescence analysis of stably transfected parasite populations revealed that both isoforms were targeted to the single *T. gondii* mitochondrion as confirmed by co-localization with the mitochondrial marker S9-GFP [21] that had been co-transfected into NDH2-myc expressing parasites (Fig. 1). We examined *tgndh2-I* and *tgndh2-II* transcript levels in the two

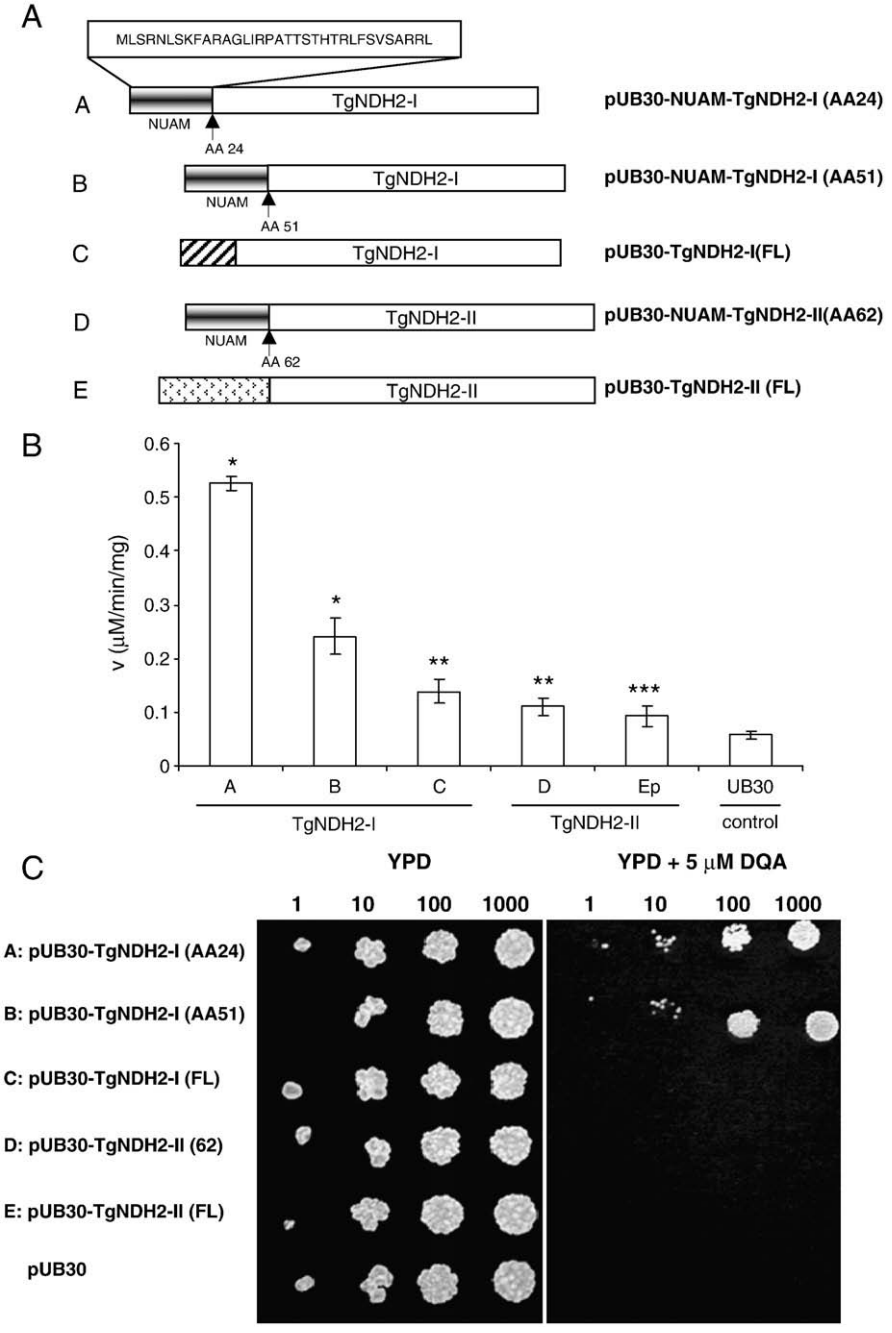

Fig. 3. TgNDH2-I displays NADH:DBQ oxidoreductase activity. (A) Schematic diagram depicting the constructs established for *Y. lipolytica* transformation. The arrows indicate the coding position for the mature parts of TgNDH2-I and TgNDH2-II. AA, amino acid; FL, full-length. (B) Oxidoreductase activity was measured in a reaction mixture containing 100 μg/ml mitochondrial membranes from *Y. lipolytica* strain GB5.2 containing pUB30-TgNDH2-I, TgNDH2-II or control pUB30 vector, 100 μM NADH and 60 μM DBQ as substrates in the presence of the complex I inhibitor DQA. Student's *t*-test; $*p<0.0001$; $**p<0.001$; $***p<0.02$ versus control pUB30 vector. (C) TgNDH2-I confers resistance to the complex I inhibitor DQA. A series of dilutions including 1, 10, 100 and 1000 cells/ml were plated on complete media in the absence or presence 5 μM DQA.

parasitic stages (tachyzoites and bradyzoites), which are present in the human host by quantitative real time RT-PCR. Both genes displayed comparable mRNA levels in the analyzed stages (Fig. 2), suggesting that they were constitutively expressed rather than stage specifically regulated.

3.2. Functional expression of TgNDH2-I in Y. lipolytica

The yeast *Y. lipolytica* expresses a single, external, non-essential NDH2 and has been established as a model organism for studying the biochemistry of alternative NADH dehydrogenases [22] and of respiratory chain complex I [23]. We used *Y. lipolytica* strain GB 5.2, in which the external NDH2 was deleted, for heterologous expression of *Tg*NDH2-I and *Tg*NDH2-II. It is not known whether a mitochondrial import sequence from a *T. gondii* protein is sufficient for accurate targeting into *Y. lipolytica* mitochondria. Thus, in addition to full-length *T. gondii* constructs, we also employed fusions of the N-terminal part of the *Y. lipolytica* mitochondrial NUAM protein and mature versions of *Tg*NDH2-I and *Tg*NDH2-II. The predicted start position for mature *Tg*NDH2-I is at amino acid 24 and for mature *Tg*NDH2-II at amino acid 62 (Fig. 3A). The predicted presequence for *Tg*NDH2-I is relatively short and after a manual sequence alignment with *Tg*NDH2-II, a second, although less likely start position for mature *Tg*NDH2-I was identified at position 51 and used for NUAM fusion. It has been demonstrated previously that the addition of the NUAM mitochondrial import signal to the external *Y. lipolytica* NDH2 is sufficient to convert this enzyme into an internal, enzymatically active isoform [18]. All constructs were placed under the control of the p*POX2* promotor in the replicative vector pUB30 [19]. Mitochondrial membrane preparations of *Y. lipolytica* transformants were analyzed for NADH dehydrogenase activity in an enzymatic assay using DBQ as electron acceptor. The NUAM-*Tg*NDH2-I fusions displayed electron transfer activities that were 10-fold (construct A: AA24) and 5-fold (construct B: AA51) higher than controls, demonstrating that this isoform can be expressed as an active enzyme in *Y. lipolytica* (Fig. 3B). Both *Tg*NDH2-II constructs displayed electron transfer activities that were less than 2-fold above controls, and the activity of full-length *Tg*NDH2-I was less than 2.5-fold above controls.

Complex I, the proton-translocating multi-subunit NADH dehydrogenase of the mitochondrial respiratory chain, is essential for growth of *Y. lipolytica*. The ability of the five expression constructs to compensate for the loss of complex I activity was tested in a *Y. lipolytica* growth assay on YPD agar plates in the presence of the complex I inhibitor DQA. Expression of *Tg*NDH2-I as NUAM fusion proteins conferred DQA resistance (Fig. 3C), in line with the results obtained from the enzyme activity assay. This demonstrated that both NUAM-*Tg*NDH2-I fusions were expressed as functional, internal enzymes with their active site oriented towards the mitochondrial matrix. NUAM-*Tg*NDH2-I expressed from construct A which displayed the highest activity and was used in all kinetic assays and is termed *Tg*NDH2i in the following.

3.3. TgNDH2i activity is effectively inhibited by 1-hydroxy-2-alkyl-4(1H) quinolones

The quinolone-like compound HDQ is a potent inhibitor of *Y. lipolytica* NDH2 [9] and our recent findings have shown that HDQ could effectively inhibit *T. gondii* replication [10]. We thus investigated the inhibitory effect of HDQ on the NADH dehydrogenase activity of *Tg*NDH2i in unsealed *Y. lipolytica* mitochondrial membranes. Using

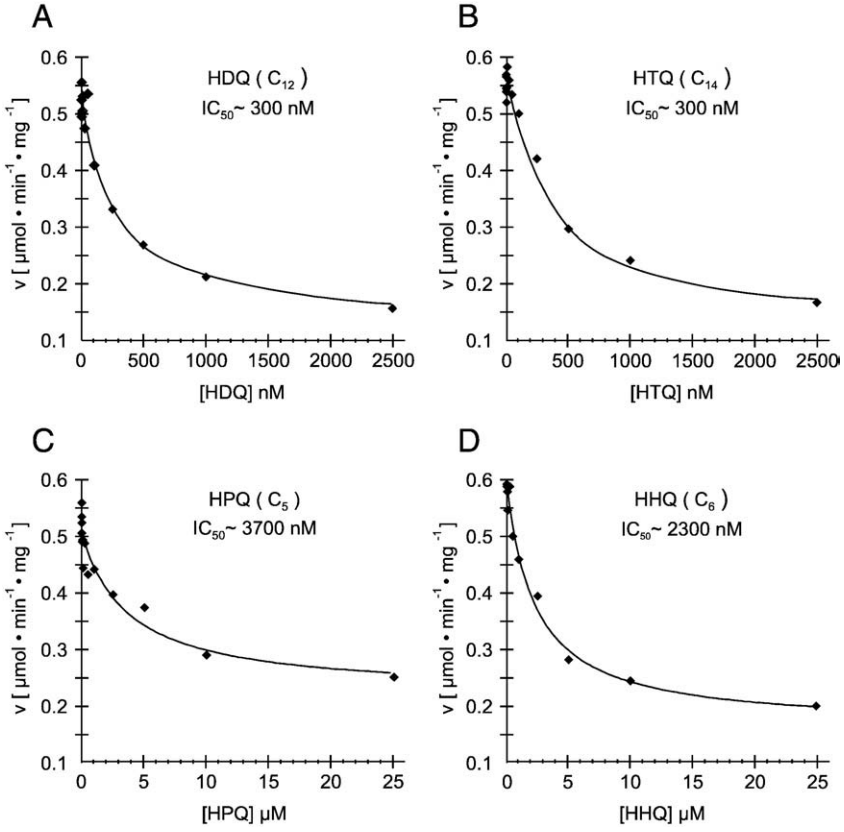

Fig. 4. Inhibition of *Tg*NDH2-I by HDQ derivatives differing in side chain length. The concentration of inhibitor required for half-maximal inhibition (IC_{50}) of *Tg*NDH2i in *Y. lipolytica* mitochondrial membranes was determined at a total protein concentration of 100 µg/ml in the presence of 60 µM DBQ and 100 µM NADH. (A–D) HDQ with C_{12}, C_{14}, C_5 and C_6 alkyl side chains, respectively.

DBQ as a substrate, inhibition of NADH:ubiquinone oxidoreductase activity by HDQ was dose dependent with a concentration required for half-maximal inhibition (IC_{50}) of about 300 nM (Fig. 4A). A 1-hydroxy-2-alkyl-4(1H)quinolone compound with a C_{14} alkyl side chain (HTQ, Fig. 4B) displayed a similar IC_{50} as HDQ (C_{12}), while derivates with shorter alkyl side chains (C_5=HPQ and C_6=HHQ) were less effective with significantly higher IC_{50} values of about 3700 nM and 2300 nM, respectively (Fig. 4C, D).

3.4. TgNDH2i bisubstrate kinetics suggest a ping-pong reaction mechanism

Mitochondrial membrane preparations from *Y. lipolytica* expressing *Tg*NDH2i were used to determine bisubstrate kinetics for NADH and DBQ. K_m values of 76 μM for NADH and 14 μM for DBQ were obtained. In a Hanes plot ([S]/v over [S]) of the kinetic data, the obtained lines crossed close to the *y*-axis (Fig. 5), which is in accordance with a ping-pong reaction mechanism for *Tg*NDH2i [9]. A (random or ordered) sequential mechanism could be excluded since in that case the lines would cross in the fourth quadrant. This result suggests that the enzyme forms binary complexes with each of the substrates, but is unable to form a ternary complex with both substrates. Most likely, both substrates interact with a common binding site in a mutually exclusive fashion.

3.5. HDQ inhibition follows a non-competitive pattern for both substrates

To determine the mode of inhibition of HDQ on *Tg*NDH2i in mitochondrial membrane preparations from *Y. lipolytica*, we performed steady-state inhibition kinetics for both NADH and DBQ. Double reciprocal plots of the kinetic data obtained in the presence of 0, 60 and 300 nM HDQ are depicted in Fig. 6. With increasing HDQ concentrations, the slopes increased, and the lines intersected close to the *y*-axis. Similar as found with *Y. lipolytica* NDH2 [9], these results formally follow the pattern of non-competitive inhibition for both substrates and similar values for the two inhibition constants (see Supplementary Fig. S2). Using linear secondary plots of the slopes and *y*-axis intercepts of the lines in Fig. 6 against the HDQ concentrations used, numeric values for the inhibition constants could be derived from the points of intersection with the *x*-axis (see Supplementary Fig. S3). Secondary plots of the slopes thus gave K_i=283 nM and K_{ii}=292 nM, and secondary plots of the intercepts gave K_i=234 nM and K_{ii}=198 nM. Within experimental error, these results are in excellent agreement with the directly determined IC_{50} value for HDQ on *Tg*NDH2i and with the assumption that K_i equals K_{ii}.

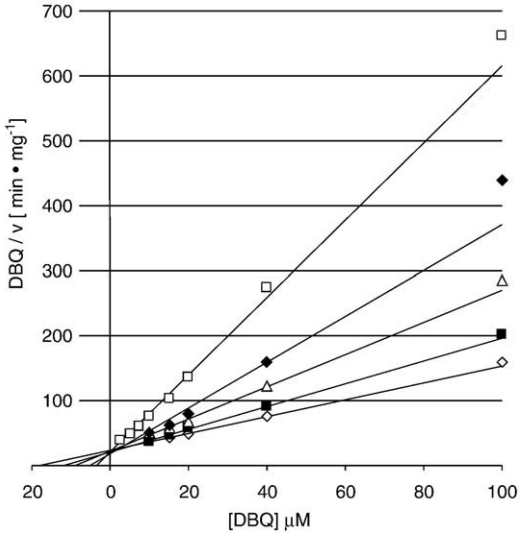

Fig. 5. *Tg*NDH2-I employs a ping-pong reaction mechanism. Hanes plots of steady-state kinetics with *Tg*NDH2i in *Y. lipolytica* mitochondrial membranes, assayed at a total protein concentration of 100 μg/ml. V_{max} and apparent K_m values for DBQ in the presence of five different NADH concentrations were obtained from direct fits to the Michaelis–Menten equation and used to draw the lines. NADH concentrations were 10 (□), 15 (♦), 30 (△), 50 (■) and 100 μM (◇). V_{max} values were 0.17±0.01 (□), 0.28±0.04 (♦), 0.40±0.04 (△), 0.57±0.06 (■) and 0.77±0.07 (◇) U/mg. Apparent K_m values were 3.5±0.5 (□), 5.3±2.9 (♦), 9.1±2.8 (△), 11.9±4.1 (■) and 18.0±5.0 μM (◇). Each data point represents the mean of five independent measurements.

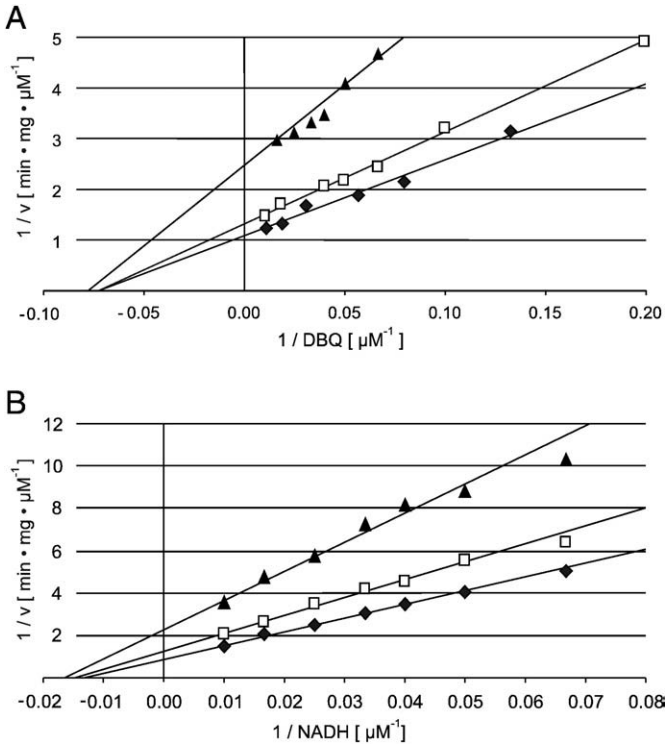

Fig. 6. Double reciprocal plots of HDQ inhibition kinetics of *Tg*NDH2i. Inhibition kinetics of *Tg*NDH2i in *Y. lipolytica* mitochondrial membranes were measured at a total protein concentration of 100 μg/ml for A, DBQ (at 100 μM NADH) and B, NADH (at 60 μM DBQ) in the absence (♦) and in the presence of 60 nM (□) and 300 nM (▲) C_{12}-HDQ. The lines for the diagrams were calculated using parameters obtained from direct fits to the Michaelis–Menten equation. In A, V_{max} values were 0.92±0.06 (♦), 0.76±0.03 (□) and 0.41±0.02 (▲) units/mg. Apparent K_m values for DBQ were 13.8±2.4 (♦), 13.8±2.0 (□) and 12.9±2.5 μM (▲). In B, V_{max} values were 1.16±0.07 (♦), 0.80±0.04 (□) and 0.44±0.03 (▲) U/mg. Apparent K_m values for NADH were 76±7 (♦), 68±5 (□) and 61±8 μM (▲). Each data point represents the mean of five independent measurements.

4. Discussion

In this study we have determined enzymatic parameters from heterologously expressed, functionally active *T. gondii* NDH2-I and could show that 1-hydroxy-2-alkyl-4(1)quinolones with long alkyl chains are high affinity inhibitors for this enzyme. *T. gondii* lacks complex I but possesses two mitochondrial type-II NADH dehydrogenases. Both are constitutively expressed, hampering direct determination of individual enzymatic parameters in *T. gondii* lysates. Thus, for *in vitro* characterization, we have expressed TgNDH2-I in a strain of the yeast *Y. lipolytica* that lacks endogenous alternative NADH dehydrogenase activity. Functional expression of TgNDH2-I as an internal NADH dehydrogenase, capable of electron transfer from matrix NADH to membrane bound ubiquinone, was achieved by fusing the TgNDH2-I open reading frame without the endogenous mitochondrial targeting sequence to the N-terminal part of the NUAM subunit of *Y. lipolytica* mitochondrial complex I. Direct evidence for *in vivo* function of TgNDH2i was provided by the observation that expression of the transgene allowed cells of *Y. lipolytica* to survive in

the presence of the complex I inhibitor DQA. Thus we were able to achieve heterologous expression of a protozoan type-II NADH dehydrogenase in an active form. Functional expression of protozoan type-II NADH dehydrogenases in *Y. lipolytica* should facilitate future comparative studies of apicomplexan orthologs. In addition, expression of protozoan type-II enzymes in *Y. lipolytica* could be used for the development of a screening assay to identify novel, specific inhibitors for this class of enzymes.

The steady-state inhibition kinetics of TgNDH2-I for the quinolone derivative HDQ were found to be very similar to those of *Y. lipolytica* NDH2 [9] and formally follow the pattern of non-competitive inhibition for both substrates, NADH and DBQ. In the case of a ping-pong reaction mechanism, this inhibition pattern is predicted when the inhibitor blocks both the enzyme, here *Tg*NDH2i-FAD and the intermediate form, here *Tg*NDH2i-$FADH_2$ [24]. As with *Y. lipolytica* NDH2 [9], our data thus support a model in which the inhibitor can interact with a complex consisting of the enzyme and one of its substrates, presumably NADH, as depicted in Supplementary Fig. S2.

Bisubstrate kinetics revealed that the NADH:DBQ oxidoreductase activity of TgNDH2i followed a ping-pong reaction mechanism, a mode of action that was also shown for the *Y. lipolytica* ortholog [9] and proposed for the *S. cerevisiae* and *T. brucei* enzymes [25,26]. The determined K_m (NADH) of 76 μM was significantly higher than the K_m of most other eukaryotic enzymes, for example from *S. tuberosum*, *N. crassa and S. cerevisiae*, which were in the range of 11–32 μM [7]. Only the *T. brucei* enzyme with 120 μM displayed a higher K_m than the *T. gondii* ortholog [26]. Also, the K_m (DBQ) of 14 μM observed for TgNDH2i was higher than the K_m (DBQ) of 7.0 μM for *Y. lipolytica* NDH2 [9]. However, differences in K_m values have to be interpreted with caution, since different electron acceptors were used in these studies and specific reaction conditions as the volume of the lipid phase could influence activities. Since the activity of TgNDH2i was about 4-fold lower than the activity of NDH2, the external alternative NADH dehydrogenase of *Y. lipolytica* parental strains, we had to double the amount of total mitochondrial protein used in the assays. Lower effective concentrations of DBQ in the lipid phase would explain the elevated K_m (DBQ) values observed in the present study. In contrast, the K_m (NADH) is not expected to depend on the volume of the lipid phase.

The IC_{50} value of about 300 nM obtained for HDQ indicates that this compound is a high affinity inhibitor for TgNDH2-I. The only other NDH2 enzyme for which the IC_{50} value for HDQ is known is the *Yarrowia* orthologue, which with 200 nM is in the same range [9]. In the future, it will be important to determine IC_{50} values for further orthologues from pathogenic and non-pathogenic microorganisms, in order to classify HDQ as a broad spectrum NDH2 inhibitor or as an inhibitor with a selected inhibitory potential. An example for a respiratory chain inhibitor with a selected inhibitory potential is the clinically approved antimalaria drug atovaquone. This drug is a complex III inhibitor that interferes with the ubiquinol oxidation site of the cytochrome bc_1 complex by acting as a competitive inhibitor for ubiquinol. Atovaquone possesses antimicrobial activity against certain apicomplexan parasites such as *Plasmodium* and *Toxoplasma* and the opportunistic fungal pathogen *Pneumocystis carinii*, whereas the human and bovine cytochrome bc_1 complexes are insensitive towards atovaquone [27].

For HDQ, the *in vitro* IC_{50} of ~300 nM for inhibition of *Tg*NDH2i activity is significantly higher than the *in vivo* IC_{50} of 2–4 nM for static effects on *T. gondii* parasites, determined in tissue culture after a 24 h treatment period [10]. Apparent differences in IC_{50} values should not be overinterpreted since these are strongly dependent on the fractional volume of the lipid phase. Assuming that a highly hydrophobic substance like HDQ will partition to the hydrophobic phase, the effective HDQ concentration for interaction with type-II NADH dehydrogenase may well differ by two orders of magnitude between the two assay systems. However, we can not exclude at present that HDQ inhibits other ubiquinone dependent NADH oxidoreductases such as succinate dehydrogenase, dihydroorotate dehydrogenase, glycerol-3-phosphate dehydrogenase and the malate: quinone oxidoreductase, in addition to type-II NADH dehydrogenases.

A long alkyl side chain of C_{12} or C_{14} at position 2 is critical for the inhibition of NADH:DBQ oxidoreductase activity. Compounds with short alkyl side chains of C_5 (HPQ) and C_6 (HHQ) with 3700 nM and 2300 nM displayed significantly higher IC_{50} values as compounds with long alkyl side chains of C_{12} (HDQ, IC_{50} = 300 nM) and C_{14} (HTQ, IC_{50} = 300 nM). On the basis of structural similarities, it is tempting to speculate that 1-hydroxy-2-alkyl-4(1H)quinolones are likely to compete with ubiquinone for the same binding site. A long alkyl site chain leads to a higher hydrophobicity and is likely to render the physicochemical properties and the structure of 1-hydroxy-2-alkyl-4 (1H)quinolones more similar to ubiquinone. Another aspect is the partition of the compounds between aqueous and membrane lipid phase. Highly hydrophobic 1-hydroxy-2-alkyl-4(1H)quinolones as HDQ and HTQ, in contrast to those with smaller alkyl side chains, can be expected to partition almost quantitatively into the membrane lipid phase. The correlation between IC_{50} values and length of the alkyl side chain mirrored the *in vivo*-efficiency of these drugs to inhibit parasite replication: HPQ (C_5) did not show any inhibitory effect at 10 nM, while parasite growth was reduced to more than 50% by HDQ and HTQ at this concentration [10]. A reevaluation of the efficiency of HHQ (C_6) to inhibit *T. gondii* replication yielded an IC_{50} of 220 nM for HHQ (C_6), which is more than 50-fold higher than the IC_{50} for HDQ (data not shown). Together, these data reveal that only 1-hydroxy-2-alkyl-4(1H)quinolones with long alkyl site chains are effective TgNDH2-I inhibitors and antiparasitic drugs.

Acknowledgments

This study has been supported by grants from the Deutsche Forschungsgemeinschaft, DFG to WB (BO 1557/3-1) and UB (SFB472, Teilprojekt P2 and EXC115). S.S. Lin is supported by a scholarship from the Croucher foundation.

Appendix A. Supplementary data

Supplementary data associated with this article can be found, in the online version, at doi:10.1016/j.bbabio.2008.08.006.

References

[1] S. Kerscher, V. Zickermann, U. Brandt, The three families of respiratory NADH dehydrogenases, Res. Probl. Cell Different 45 (2008) 185–222.
[2] U. Brandt, Energy converting NADH quinone oxidoreductases, Annu. Rev. Biochem. 75 (2006) 69–92.
[3] J. Carroll, I.M. Fearnley, R.J. Shannon, J. Hirst, J.E. Walker, Analysis of the subunit composition of complex I from bovine heart mitochondria, Mol. Cell. Proteomics 2 (2003) 117–126.
[4] M. Radermacher, T. Ruiz, T. Clason, S. Benjamin, U. Brandt, V. Zickermann, The three-dimensional structure of complex I from *Yarrowia lipolytica*: a highly dynamic enzyme, J. Struct. Biol. 154 (2006) 269–279.
[5] D. Elhafez, M.W. Murcha, R. Clifton, K.L. Soole, D.A. Day, J. Whelan, Characterization of mitochondrial alternative NAD(P)H dehydrogenases in *Arabidopsis*: intraorganelle location and expression, Plant Cell Physiol. 47 (2006) 43–54.
[6] K.M. Overkamp, B. Bakker, P. Kötter, A. van Tuijl, S. de Vries, J.P. van Dijken, J.T. Pronk, In vivo analysis of the mechanisms for oxidation of cytosolic NADH by *Saccharomyces cerevisiae* mitochondria, J. Bacteriol. 182 (2000) 2823–2830.
[7] A.M. Melo, T.M. Bandeiras, M. Teixeira, New insights into type II NAD(P)H:quinone oxidoreductases, Microbiol. Mol. Biol. Rev. 68 (2004) 603–616.
[8] G.A. Biagini, P.O. Viriyavejakul, P.M. O'Neill, P.G. Bray, S.A. Ward, Functional characterization and target validation of alternative complex I of *Plasmodium falciparum* mitochondria, Antimicrob. Agents Chemother. 50 (2006) 1841–1851.
[9] A. Eschemann, A. Galkin, W. Oettmeier, U. Brandt, S. Kerscher, HDQ (1-hydroxy-2-dodecyl-4(1H)quinolone) a high affinity inhibitor for mitochondrial alternative NADH dehydrogenase, J. Biol. Chem. 280 (2005) 3138–3142.
[10] A. Saleh, J. Friesen, S. Baumeister, U. Gross, W. Bohne, Growth inhibition of *Toxoplasma gondii* and *Plasmodium falciparum* by nanomolar concentrations of 1-hydroxy-2-dodecyl-4(1H)quinolone a high-affinity inhibitor of alternative (type II) NADH dehydrogenases, Antimicrob. Agents Chemother. 51 (2007) 1217–1222.

[11] J.C. Kissinger, B. Gajria, I.T. Paulsen, D.S. Roos, ToxoDB: accessing the *Toxoplasma gondii* genome, Nucleic Acids Res. 31 (2003) 234–236.
[12] D.S. Roos, R.G. Donald, N.S. Morrissette, A.L. Moulton, Molecular tools for genetic dissection of the protozoan parasite *Toxoplasma gondii*, Methods Cell Biol. 45 (1994) 27–63.
[13] M. Meissner, D. Schluter, D. Soldati, Role of *Toxoplasma gondii* myosin A in powering parasite gliding and host cell invasion, Science 298 (2002) 837–840.
[14] M. Soete, D. Camus, J.F. Dubremetz, Experimental induction of bradyzoite-specific antigen expression and cyst formation by the RH strain of *Toxoplasma gondii* in vitro, Exp. Parasitol. 78 (1994) 361–370.
[15] M. Meissner, S. Brecht, H. Bujard, D. Soldati, Modulation of myosin A expression by a newly established tetracycline repressor-based inducible system in *Toxoplasma gondii*, Nucleic Acids Res. 29 (2001) E115.
[16] R.G. Donald, D.S. Roos, Stable molecular transformation of *Toxoplasma gondii*: a selectable dihydrofolate reductase-thymidylate synthase marker based on drug-resistance mutations in malaria, Proc. Natl. Acad. Sci. U. S. A. 90 (1993) 11703–11707.
[17] M.T. Black, F. Seeber, D. Soldati, K. Kim, J.C. Boothroyd, Restriction enzyme-mediated integration elevates transformation frequency and enables co-transfection of *Toxoplasma gondii*, Mol. Biochem. Parasitol. 74 (1995) 55–63.
[18] S. Kerscher, A. Eschemann, P.M. Okun, U. Brandt, External alternative NADH: ubiquinone oxidoreductase redirected to the internal face of the mitochondrial inner membrane rescues complex I deficiency in *Yarrowia lipolytica*, J. Cell. Sci. 114 (2001) 3915–3921.
[19] A. Garofano, A. Eschemann, U. Brandt, S. Kerscher, Substrate-inducible versions of internal alternative NADH:ubiquinone oxidoreductase from *Yarrowia lipolytica*, Yeast 23 (2006) 1129–1136.
[20] S. Kerscher, J.G. Okun, U. Brandt, A single external enzyme confers alternative NADH:ubiquinone oxidoreductase activity in *Yarrowia lipolytica*, J. Cell. Sci. 112 (1999) 2347–2354.
[21] A. DeRocher, C.B. Hagen, J.E. Froehlich, J.E. Feagin, M. Parsons, Analysis of targeting sequences demonstrates that trafficking to the *Toxoplasma gondii* plastid branches off the secretory system, J. Cell. Sci. 113 (2000) 3969–3977.
[22] S. Kerscher, Diversity and origin of alternative NADH:ubiquinone oxidoreductases, Biochim. Biophys. Acta 1459 (2000) 274–283.
[23] S. Kerscher, S. Dröse, K. Zwicker, V. Zickermann, U. Brandt, *Yarrowia lipolytica* a yeast genetic system to study mitochondrial complex I, Biochim. Biophys. Acta 1555 (2002) 83–91.
[24] W.W. Cleland, The kinetics of enzyme-catalyzed reactions with two or more substrates or products. III. Prediction of initial velocity and inhibition patterns by inspection, Biochim. Biophys. Acta 67 (1963) 188–196.
[25] I. Velazquez, J.P. Pardo, Kinetic characterization of the rotenone-insensitive internal NADH:ubiquinone oxidoreductase of mitochondria from *Saccharomyces cerevisiae*, Arch. Biochem. Biophys. 389 (2001) 7–14.
[26] J. Fang, D.S. Beattie, Novel FMN-containing rotenone-insensitive NADH dehydrogenase from *Trypanosoma brucei* mitochondria: isolation and characterization, Biochemistry 41 (2002) 3065–3072.
[27] A.L. Baggish, D.R. Hill, Antiparasitic agent atovaquone, Antimicrob. Agents Chemother. 46 (2002) 1163–1173.